

## PAPER DETAILS

TITLE: A Broadband Suspended Plate Antenna with Dual Polarization for 2G/3G/Wi-Fi/4G/LTE

AUTHORS: Emre Alp Miran,Burak Uzman,Tayfun Okan

PAGES: 1205-1213

ORIGINAL PDF URL: <https://dergipark.org.tr/tr/download/article-file/3345514>



## A Broadband Suspended Plate Antenna with Dual Polarization for 2G/3G/Wi-Fi/4G/LTE

Emre A. MIRAN<sup>1</sup> , Burak UZMAN<sup>2</sup> , Tayfun OKAN<sup>3</sup>

<sup>1</sup> ESEN System Integration, 06800, Ankara, Türkiye

<sup>2</sup> ENGITEK Engineering Ltd. 06200, Ankara, Türkiye

<sup>3</sup> TAI - Turkish Aerospace Industries, Inc. 06980, Ankara, Türkiye

### Highlights

- This paper focuses on design of a dual polarized broadband base station antenna in 1710-2690 MHz.
- Suspended plate antenna with parasitic patch has been excited by crossed elliptic-slots.
- A low profile and high isolation antenna is achieved for desired electrical performance.

### Article Info

Received: 19 Aug 2023  
Accepted: 14 Dec 2023

### Keywords

Dual-polarization  
Broadband  
2G/3G/Wi-Fi/4G/LTE  
Suspended plate  
Base station antenna

### Abstract

Design of a broadband, dual-polarized suspended patch antenna covering 2G/3G/Wi-Fi/4G bands (1710-2690 MHz) is presented. The prototype consists of two suspended plates and a feedline layer. Excitation of  $\pm 45^\circ$  slant dual polarization is realized by a novel crossed elliptic-H slot. The prototype exhibits 48.7% impedance bandwidth ( $|S_{11}|, |S_{22}| < -15$  dB) in 1660-2730 MHz. Port isolation ( $|S_{21}|$ ) is obtained as  $> 28$  dB. In desired operating band, stable and symmetric radiation patterns with half-power beamwidths of  $55^\circ$ - $75^\circ$  and  $65^\circ$ - $74^\circ$  in E and H planes are measured, respectively. Gain variation lies within  $8.3 \pm 0.8$  dBi. Proposed antenna is low profile, has high port isolation and high front to back ratio without needing any secondary reflector ground plane. With these qualifications and performance specifications, it outperforms many of the similar works in the literature. Design considerations, simulations and measurement results of proposed antenna are presented and discussed.

## 1. INTRODUCTION

In recent years, mobile cellular industry has started to deploy multiband 2G/3G/4G/LTE radios and antennas in most part of the radio access network to avoid cumbersome installations and reduce cost. Hence researchers have been working on antennas spanning 2G/3G/4G/LTE frequency bands, i.e., GSM1800 (1710-1880MHz), 3G/UMTS (1910-2170 MHz) and 4G/LTE (2490-2690 MHz). Moreover, it is also desirable to cover 2400MHz ISM band for Wi-Fi base stations. Design of such dual-polarized base station antennas has focused on being low profile, broad impedance bandwidth (IBW), high port isolation, directional and stable radiation pattern with sufficient gain, high front to back ratio (FBR) and high cross polar discrimination (XPD) level.

In these developmental works, there are mainly two types of antennas employed or studied. Majority of them are crossed-dipoles having a pair of dipoles with  $\pm 45^\circ$  orientation [1-4]. Although they provide reliable, satisfactory solutions and high polarization isolation, they have high profile and complex feeding structure with balun. Magneto-electric dipoles reported in [5-7] can also be regarded as crossed-dipoles. The other common type is planar patch antennas. Although many methods have been developed to overcome their narrow band nature of patches, they have not attracted as much interest as crossed-dipoles in the design of base station antennas, maybe because of the difficulty to cover the entire band (1710-2690 MHz). Printed microstrip patch has narrow bandwidth and hence suspended patch or suspended stacked patches can be used for broadband operation for base station antennas. Patch antennas are fed or excited,

in general, by capacitive coupling probe [8-12] or slot coupling [13-19]. In [8], a patch antenna with anti-symmetric L-shaped probe feeds printed on a dielectric substrate is presented in [8]. In [9], a stacked patch antenna fed by F-shaped probes is proposed. [13] also reports a stacked patch antenna, which is excited by separate rectangular slots. But it is not capable of maintaining the port isolation above 20 dB in the desired band. Design of a novel stacked patch antenna fed by modified H-slots in crossed configuration for dual polarization is presented in [14]. Although it exhibits high isolation, only GSM1800 and 3G/UMTS bands are covered. Suspended patch antennas excited by slots in multilayers has been proposed by [15-17]. However, they are also not able to cover the entire 2G/3G/Wi-Fi/4G/LTE frequency bands (1710-2690 MHz). Moreover, slot coupled patch antennas, in general, are simple but high profile because they may need an additional reflector plane, or a cavity backed structure, or some back spacers/scatterers to have high FBR, which increases overall antenna profile as in the works of [6, 7]. [18, 19] are also examples of low-profile slot coupled patch antennas without reflector in 5G band (3300-3800 MHz) for base stations. They exhibit narrower IBW (typically 20-25%) with different patch configurations.

Table 1 summarizes and compares some of the prominent related designs with this work. In this table, [3, 4] are crossed-dipoles, and [6, 7] are magneto-electric dipoles. [8, 9] are patch/plate antennas with probe fed excitations, and [13-17] are patch/plate antennas with slot coupling. This work falls in the same category with [13-17].

**Table 1.** Literature summary and comparison of similar studies

Ref.	Antenna Type	IBW (GHz, %) < [dB]	Isolation	FBR	XPD <sup>2</sup>	Height
[3]	Crossed Dipole	1.71-2.69, 44.6% < -15	> 25 dB	> 30 dB	> 20 dB	41 cm
[4]	Crossed Dipole	1.70-2.90, 52.2% < -15	> 25 dB	> 40 dB	> 18 dB	34 cm
[6]	Magneto-electric Dipole	0.98-1.90, 64% < -10	> 37 dB	> 20 dB	> 40 dB	48 cm
[7]	Magneto-electric Dipole	1.62-2.87, 56% < -15	> 30 dB	> 20 dB	> 20 dB	48 cm
[8]	Probe-fed Patch	1.71-2.83, 49.3% < -10	> 30 dB	> 40 dB	> 25 dB	32 cm
[9]	Probe-fed Patch	1.71-2.71, 45% < -15	> 28 dB	> 22 dB	> 23 dB	32 cm
[13]	Slot-coupled Patch with Reflector	1.92-2.69, 33.4% < -10	> 16 dB	N/A <sup>1</sup>	> 25 dB	34.4 cm
[14]	Slot-coupled Patch with Reflector	1.62-2.25, 32.5% < -15	> 33 dB	> 25 dB	N/A	57.3 cm
[15]	Slot-coupled Patch	2.39-2.95, 20.9% < -10	> 35 dB	> 21 dB	> 22 dB	12 cm
[16]	Slot-coupled Patch with Reflector	1.69-2.21, 26.6% < -10	> 25 dB	> 30 dB	> 20 dB	29.6 cm
[17]	Slot-coupled Patch	2.44-3.14, 25.1% < -10	> 20 dB	> 24 dB	> 25 dB	11 cm
This Work	Slot-coupled Patch	1.60-2.80, 54.5% < -10 1.66-2.73, 48.7% < -15	> 28 dB	> 30 dB	> 27 dB	26.6 cm

<sup>1</sup> N/A: not applicable, <sup>2</sup> :XPD levels are taken at boresight ( $\theta = 0^\circ$ ).

In this work, the design of a broadband, dual-polarized suspended patch antenna to operate in 1710-2690 MHz is reported in a simple configuration. Proposed antenna consists of two suspended patches: main patch and parasitic patch. Excitation of the patches is realized by coupling the electromagnetic power through orthogonally placed ( $\pm 45^\circ$ ) crossed elliptic-H slots. In addition to proper placement of patches, slot geometry is also another factor to have broadband nature of antenna. Proposed antenna has -15 dB impedance BW of 48% in 1660-2730 MHz and -10 dB impedance BW of 54%. Port isolation is obtained to be > 28 dB in the desired band. Half-power beamwidths (HPBW<sub>s</sub>) are measured to be 55°-75° and 65°-74° in E and H planes respectively with a gain variation of 8.3±0.8 dBi. Proposed design is also low profile with high FBR (> 30 dB) without using any additional reflector, a cavity backed structure, or some back spacers/scatterers. Low XPD level is also achieved (> 27 dB).

Research presentation is organized as follows. Section 2 mentions antenna design with geometry, configuration, simulations and numerical studies. Experimental results are presented in section 3. Then discussion and conclusion are provided in section 4.

## 2. MATERIAL METHOD

### 2.1. Antenna Geometry

The proposed antenna comprises two suspended metal patches and a feedline layer. The patches are 0.5 mm thick square metal sheets, with the main patch, which is of length  $L_{mp}$ , mounted on top of the feedline

layer at a height of  $h_{mp}$ . The parasitic patch, which is of length  $L_{pp}$ , is separated from the main patch by an air layer of height  $h_{pp}$ . The main patch is rotated by  $45^\circ$  around its axis in order to create two orthogonal linear polarizations along  $\pm 45^\circ$ . The feeding network is located at the bottom of the FR4 layer of 1.6 mm thickness with a dielectric constant of  $\epsilon_r = 4.4$  and a dielectric loss of  $\tan\delta = 0.02$ . The slots are etched on top of the FR4 layer. The Antenna is fed through  $50\ \Omega$  microstrip lines connected to SMA connectors. Feeding lines are positioned at the bottom to produce  $\pm 45^\circ$  polarization diversity, with an air bridge to prevent overlap at the crossing point. Electromagnetic energy is coupled to slots using two  $100\ \Omega$  parallel branch lines. A T-junction is utilized as 1-to-2 power divider to connect the main feeding lines to the branch lines, which are terminated with L-shaped open-ended stubs. The design incorporates crossed elliptic-H slots rather than traditional rectangular-H slots, where the slot center is redesigned to be an ellipse, resulting in an improvement in port isolation and IBW. The antenna geometry and feed structure are shown in Figure 1, and the physical dimensions are presented in Table 2.

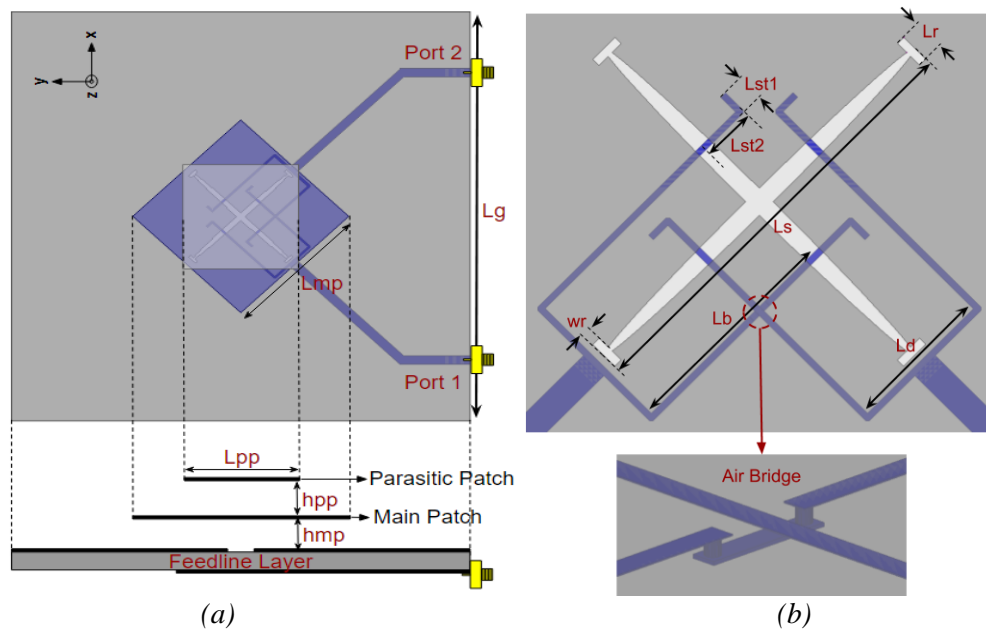


**Figure 1.** Proposed antenna: a) Geometry, b) feed structure

**Table 2.** Antenna Dimensions

Description	Parameter	Dimension (mm)
Ground size (square)	$L_g$	150
Lower patch size (square)	$L_{mp}$	52
Upper patch size (square)	$L_{pp}$	40
Lower air layer height	$h_{mp}$	12
Upper air layer height	$h_{pp}$	12
Slot length	$L_s$	45
Vertical slot length and width	$L_r, W_r$	3.2, 0.9
Stub length #1	$L_{st1}$	5.55
Stub length #2	$L_{st2}$	2.1
Branch Line Length	$L_b$	24
Branch Separation	$L_d$	15.33
Patch sheet thickness	$d$	0.5
FR4 height	$h$	1.6
Overall height		$h_{mp} + h_{pp} + (2 \times d) + h = 26.6$

## 2.2. Numerical Studies

Antenna design and development has been performed by Ansoft HFSS simulation software in order to optimize its electrical performance. In the simulations, one parameter was varied by sweeping values within a specific range while keeping the remaining parameters constant. Due to the compact and symmetrical structure of the antenna, only three main parameters, namely  $h_{mp}$ ,  $h_{pp}$ , and the axial ratio of the ellipse ( $A_{xr}$ ), were investigated for their effects on impedance matching ( $|S_{11}|$ ) and port isolation ( $|S_{21}|$ ). Simulations for the second port ( $|S_{22}|$ ) were not presented due to symmetric structure of the antenna. The lower/upper boundaries of the operating band (1710-2690 MHz) are indicated by vertical dashed lines in the plots. Figure 2 depicts the variation of  $|S_{11}|$  and  $|S_{21}|$  with the main patch height  $h_{mp}$ , which is varied from 10 mm to 14 mm in steps of 1 mm. The largest impedance bandwidth (IBW) is achieved when  $h_{mp}$  is set to 12 mm, where two resonance points are observed at 1764 MHz and 2604 MHz. The isolation between the ports is above 30 dB in the targeted operating band. Similar results are obtained for the parasitic patch height  $h_{pp}$ , as shown in Figure 3. The largest IBW is achieved when  $h_{pp} = 11$  mm, but better impedance matching is attained when  $h_{pp} = 12$  mm. When  $h_{pp}$  is increased above 12 mm, the IBW and matching level degrade. The highest port isolation in the 1710-2690 MHz band is also achieved when  $h_{pp} = 12$  mm. The effect of the parasitic patch on the overall antenna performance is investigated for  $h_{mp} = 12$  mm and  $h_{pp} = 12$  mm, as shown in Figure 4. The desired operating band for 2G/3G/Wi-Fi/4G/LTE (1710-2690 MHz) cannot be covered without the parasitic patch for  $|S_{11}| < -15$  dB or even for  $|S_{11}| < -10$  dB. Without the parasitic patch, the overall height of the antenna can be reduced to 14.1 mm, but the IBW performance deteriorates and becomes comparable to that of related works in Table 1. However, with the parasitic patch, the overall height becomes 26.6 mm, which is still the minimum among related works in Table 1, and the percent IBW performance improves, covering the entire desired band and exceeding the performance of related works in Table 1. Therefore, the parasitic patch is essential despite increasing the overall height of the antenna.

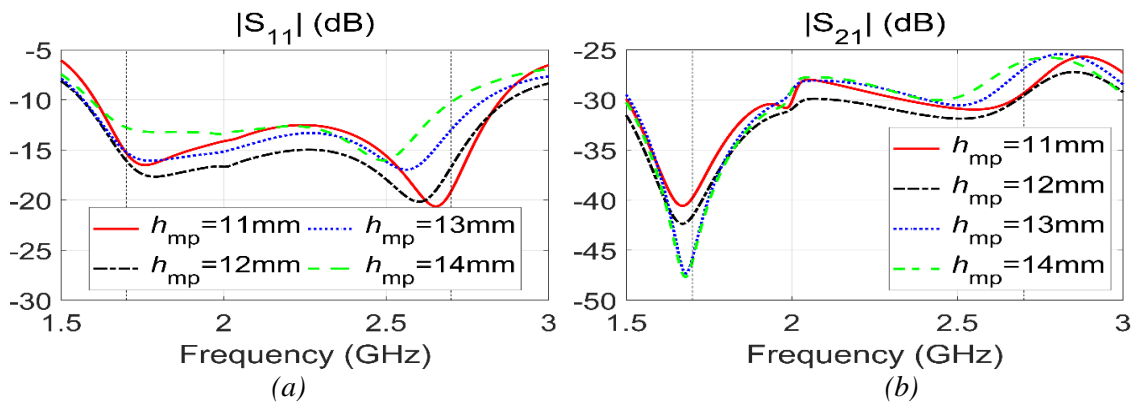


**Figure 2.** Effect of  $h_{mp}$  (a)  $|S_{11}|$  reflection, (b)  $|S_{21}|$  isolation

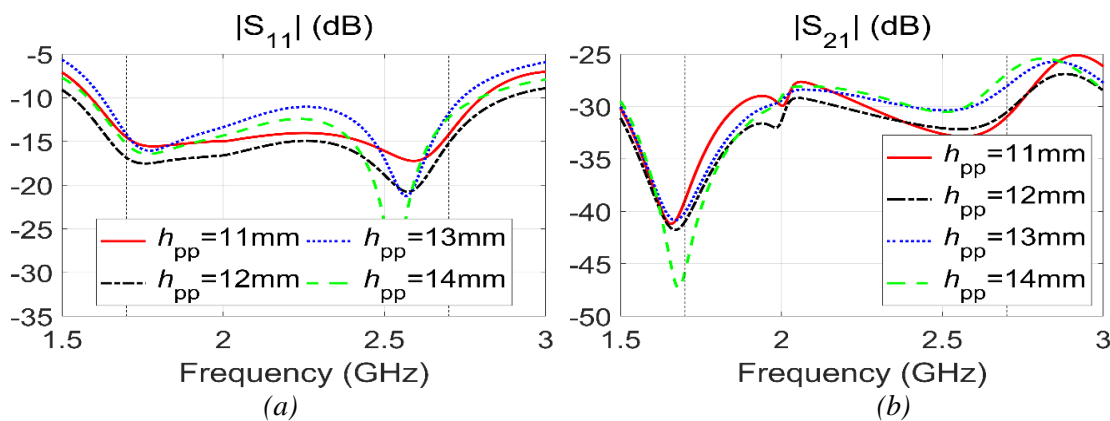


**Figure 3.** Effect of  $h_{pp}$  (a)  $|S_{11}|$  reflection, (b)  $|S_{21}|$  isolation

In Figure 5,  $|S_{11}|$  and  $|S_{21}|$  are plotted as a function of  $A_{xr}$ . The axial ratio is varied from 20 to 23.75 in steps of 1.25. The antenna exhibits the best matching level when  $A_{xr} = 20$ , with resonance points at 2130 MHz and 2538 MHz. However, it fails to cover the entire 1710-2690 MHz band, providing only 38.64%  $-15$  dB IBW. On the other hand, when  $A_{xr}$  is set to 22.5, the antenna achieves its largest IBW with a considerably good level of matching as well. The resonance points are obtained at 1758 MHz and 2592 MHz, and the isolation level is seen to be greater than 29.5 dB.

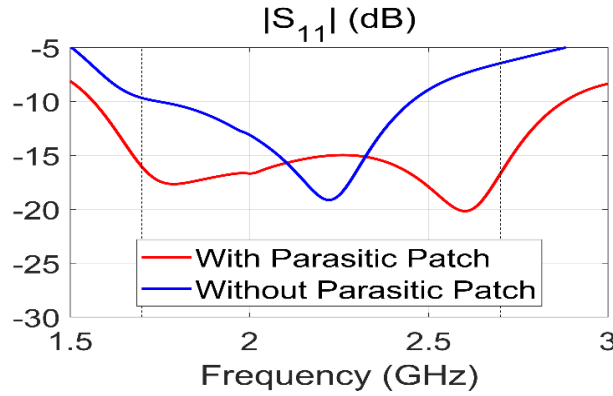


**Figure 4.** Effect of presence of parasitic patch

The advantage of using an elliptic-H slot on the electrical performance of the antenna is demonstrated by comparing it with a rectangular-H slot of the same length ( $L_s = 45$  mm) and area ( $A_s \cong 282$  mm<sup>2</sup>). The results of this comparison are presented in Figure 6. The tapered structure of the elliptic-H slot makes it more suitable for broadband matching, resulting in more efficient energy transfer from the slots to the patches, as shown in Figure 6(a). Additionally, weaker current distribution flows on the elliptic-H slots plane when compared to that of the rectangular slot, as demonstrated in Figure 6(b). Due to low level current between the ports, particularly around the center region where the majority of coupling occurs, lower mutual coupling and stronger port isolation are achieved.

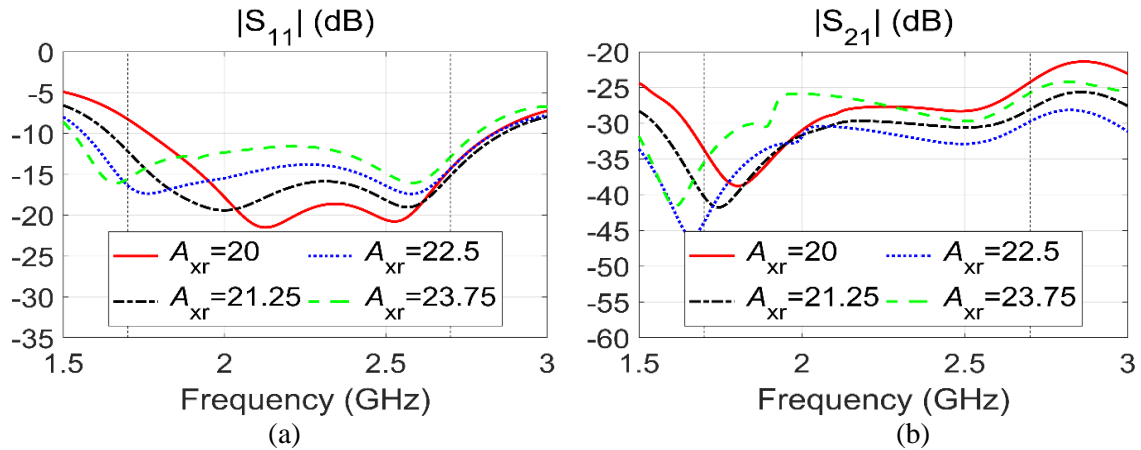


**Figure 5.** Effect of  $A_{xr}$  (a)  $|S_{11}|$  reflection, (b)  $|S_{21}|$  isolation

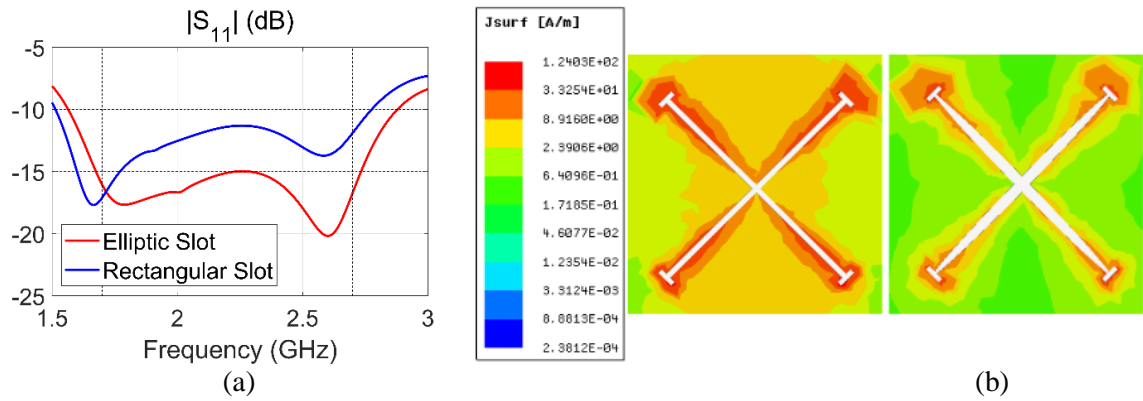


**Figure 6.** Comparison of elliptic and rectangular-H slot in terms of a)  $|S_{11}|$ , b) current distribution

### 3. EXPERIMENTAL RESULTS

To verify the accuracy of the simulation results, the proposed design, outlined in section 2 and depicted in Figure 7, is prototyped. Performance of the prototype is evaluated by measuring its S-parameters ( $|S_{11}|$ ,  $|S_{22}|$ ,  $|S_{21}|$ ) using an HP 8720D vector analyzer, as well as its radiation patterns in an anechoic chamber.

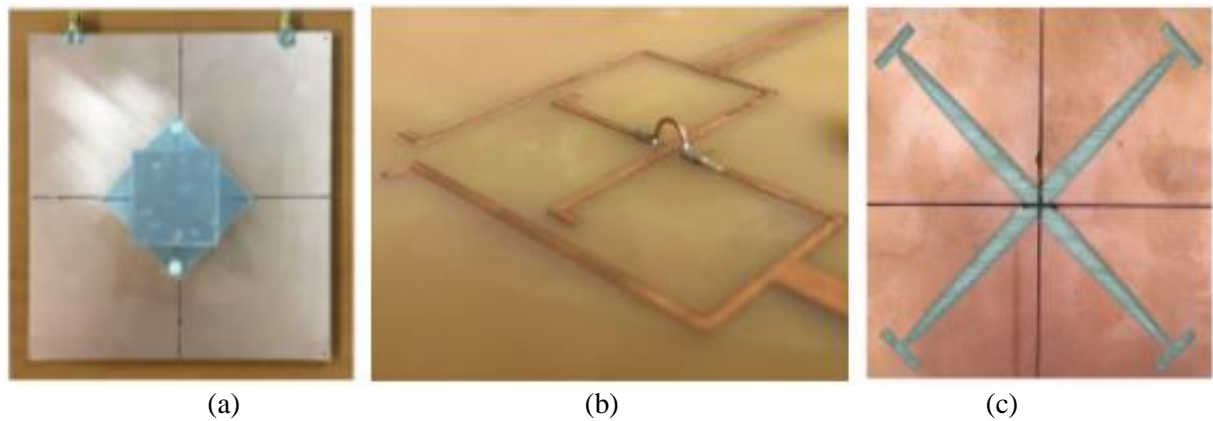


**Figure 7.** Prototype antenna (a) top view, (b) feed network, (c) elliptic-H slots

Simulated and measured S-parameters are consistent with each other and depicted in Figure 8. Prototype exhibits -10 dB IBW in 1600-2800 MHz (54.5%) and -15 dB IBW in 1660-2730 MHz (48.7%) with two resonance points at 1609 MHz and 2795 MHz. Port isolation is measured above 28 dB (typ. > 30 dB) along the desired band.

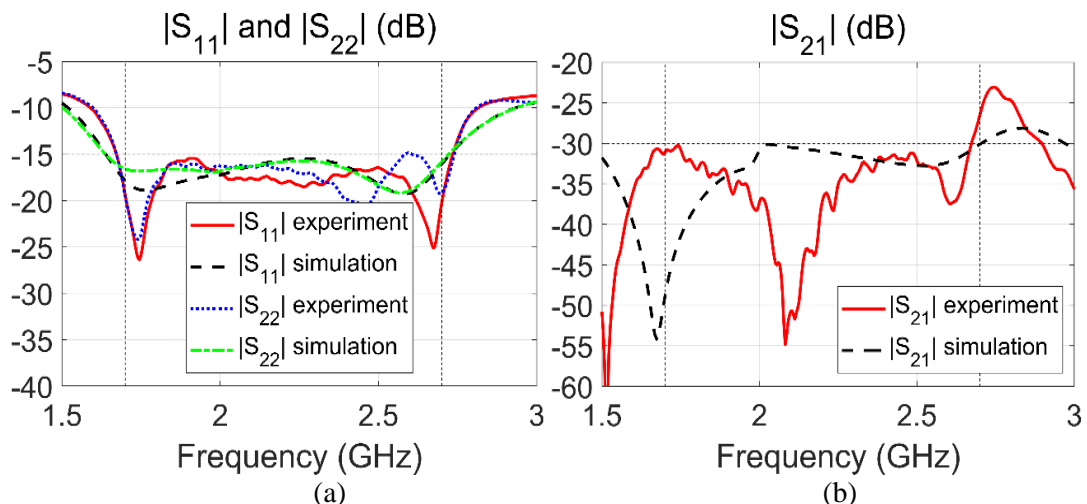


**Figure 8.** Simulated and measured S-parameters. a)  $|S_{11}|$ ,  $|S_{22}|$ , and b)  $|S_{21}|$

Regarding radiation patterns, normalized co/cross-pol components in E and H planes are illustrated in Figure 9 at 1700 MHz, 2200 MHz, and 2700 MHz. Prototyped antenna provides symmetric, broadside radiation patterns in the entire band with HPBW of 75°, 66°, and 55° in E plane and 74°, 69°, and 65° in H plane at corresponding frequencies respectively. Simulated and measured radiation patterns indicate that designed antenna has FBR > 30 dB and XPD > 27 dB. Gain of the antenna is about 8.3±0.8 dBi and plotted in Figure 10.

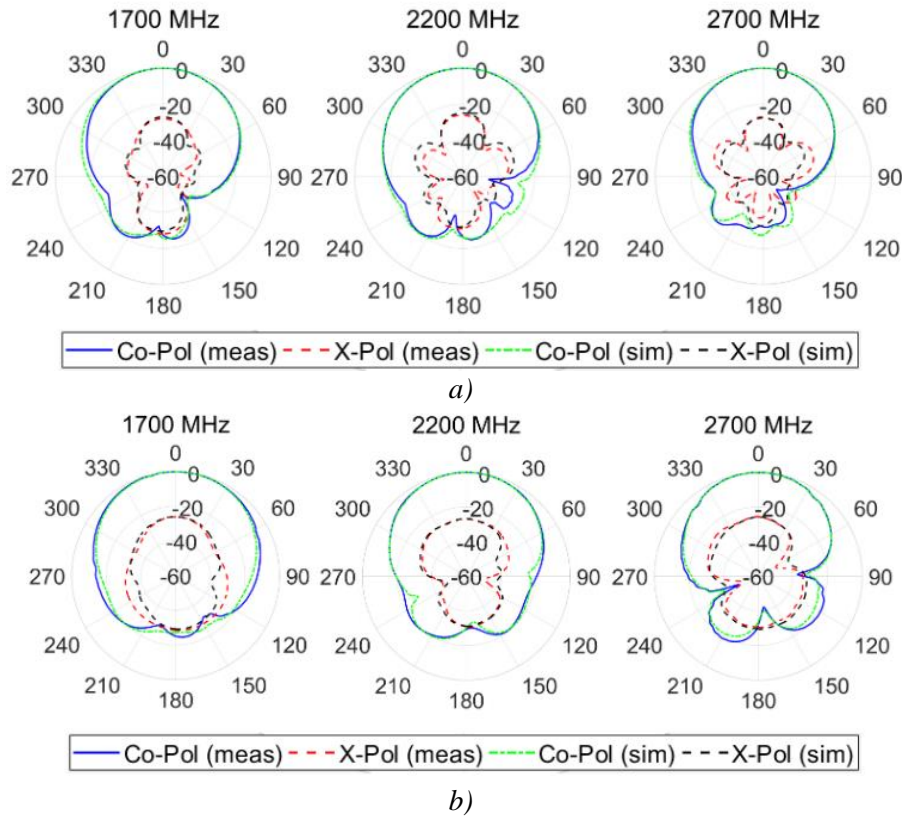


**Figure 9.** Co/Cross-pol radiation patterns in (a) E-plane and (b) H-plane

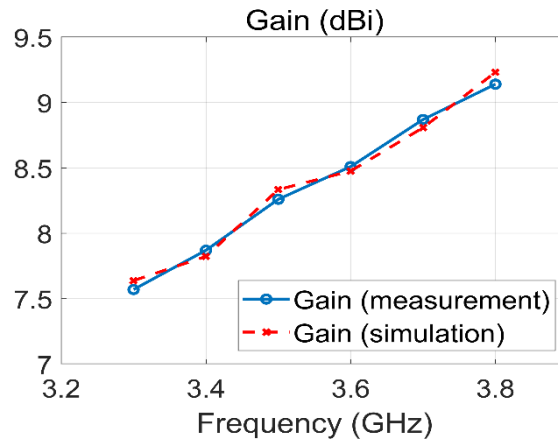


**Figure 10.** Simulated and measured gain of the antenna

#### 4. CONCLUSION

This paper presents the design of a suspended patch antenna for use in 2G/3G/Wi-Fi/4G/LTE base stations that is simple, low-cost, low-profile, broadband, and dual-polarized. The antenna's feeding mechanism is achieved using crossed elliptic-H slots for  $\pm 45^\circ$  dual polarization, which allows for broadband operation, and the proper placement of stacked patches. As a result, the antenna spans the entire 2G/3G/Wi-Fi/4G/LTE band with very good matching and port isolation. The prototyped antenna has a HPBW of 55°-75° and 65°-

74° in the E and H planes, respectively, with a gain variation of  $8.3 \pm 0.8$  dBi. The antenna also has an XPD level and FBR of  $> 27$  dB and  $> 30$  dB, respectively, and does not require an additional reflector or cavity backed structure, making it low profile. The proposed antenna satisfies all the base station antenna requirements simultaneously and outperforms other designs given in Table 1. Based on the numerical and measurement results, the proposed antenna can be used in the array design of base station antennas for 2G/3G/Wi-Fi/4G/LTE applications.

## ACKNOWLEDGMENT

This project is partially funded by The Scientific and Technological Research Council of Turkey (TUBITAK) under Grant No. 3201110.

## CONFLICTS OF INTEREST

No conflict of interest was declared by the authors.

## REFERENCES

- [1] Ta, S. X., Park, I., and Ziolkowski, R.W., “Crossed dipole antennas: A review”, *IEEE Antennas and Propagations Magazine*, 57(5): 107-122, (2015).
- [2] Ding, C., Sun, H., Ziolkowski, R.W., and Guo, Y. J., “Simplified tightly-coupled cross-dipole arrangement for base station applications”, *IEEE Access*, 5: 27491–27503, (2017).
- [3] Luo, Y., Chu, Q. X., and Wen, D. L., “A plus/minus 45-degree dual-polarized base-station antenna with enhanced cross-polarization discrimination via addition of four parasitic elements placed in a square contour”, *IEEE Transactions on Antennas and Propagation*, 64(4): 1514–1519, (2016).
- [4] Wen, D. L., Zheng, D. Z., and Chu, Q. X., “A wideband differentially fed dual-polarized antenna with stable radiation pattern for base stations”, *IEEE Transactions on Antennas and Propagation*, 65(5): 2248–2255, (2017).
- [5] Wu, B. Q., Luk, K. M., “A broadband dual-polarized magneto-electric dipole antenna with simple feeds”, *IEEE Antennas and Wireless Propagation Letters*, 8: 60–63, (2009).
- [6] Xue, Q., Liao, S.W., and Xu, J. H., “A differentially-driven dual-polarized magneto-electric dipole antenna”, *IEEE Transactions on Antennas and Propagation*, 61(1): 425–430, (2013).
- [7] Zhou, S. G., Peng, Z. H., Huang, G. L., and Sim, C.Y.D., “Design of a novel wideband and dual-polarized magneto-electric dipole antenna”, *IEEE Transactions on Antennas and Propagation*, 65(5): 2645–2649, (2017).
- [8] Mak, K. M., Lai, H.W., and Luk, K. M., “A 5G wideband patch antenna with antisymmetric L-shaped probe feeds”, *IEEE Transactions on Antennas and Propagation*, 66(2): 957–961, (2018).
- [9] Jin, Y., Du, Z., “Broadband dual-polarized F-probe fed stacked patch antenna for base stations”, *IEEE Antennas and Wireless Propagation Letters*, 14: 1121–1124, (2015).
- [10] Ciydem, M., “Wideband dual polarized antenna”, *Journal of the Faculty of Engineering and Architecture of Gazi University*, 29(4): 817-821, (2014).
- [11] Ciydem, M., “Isolation enhancement in wideband dual-polarised suspended plate antenna with modified T-type probes,” *Electronics Letters*, 50(5): 338-339, (2014).

- [12] Ali, A., Ciydem, M., Altintas, A., Koc, S., “VHF suspended plate transmitter antenna design for DVB-T and DAB-T”, *Microwave and Optical Technology Letters*, 60(6): 1536-1546, (2018).
- [13] Serra, A. A., Nepa, P., Manara, G., Tribellini, G., and Cioci, S., “A wideband dual-polarized stacked patch antenna”, *Antennas and Wireless Propagation Letters*, 6: 141–143, (2007).
- [14] Barba, M., “A high isolation, wideband and dual linear polarization patch antenna”, *IEEE Transactions on Antennas Propagation*, 56(5): 1472–1476, (2008).
- [15] Gao, S. C., Li, L.W., Leong, M. S., and Yeo, T.S., “Dual-polarized slot-coupled planar antenna with wide bandwidth”, *IEEE Transactions on Antennas Propagation*, 51(3): 441–448, (2003).
- [16] Wang, Y., Du, Z., “Dual-polarized slot-coupled microstrip antenna array with stable active element pattern”, *IEEE Transactions on Antennas and Propagation*, 63(9): 4239–4244, (2015).
- [17] Gao, S. C., Li, L. W., Leong, M. S., and Yeo, T. S., “A broadband dual-polarized microstrip patch antenna with aperture coupling”, *IEEE Transactions on Antennas and Propagation*, 51(4): 898-900, (2003).
- [18] Ciydem, M., “A low-profile dual-polarized antenna with high isolation and high front-to-back ratio for 5G base stations”, *The Applied Computational Electromagnetics Society Journal (ACES)*, 36(9): 1229-1236, (2021).
- [19] Miran, E. A., Ciydem, M., “Dual-polarized elliptic-H slot-coupled patch antenna for 5G applications”, *Turkish Journal of Electrical Engineering and Computer Sciences*, 30(4): 1204-1218, (2022).